

Proton decay testing low energy SUSY

Stefan Pokorski,^{1,2} Krzysztof Rolbiecki,¹ and Kazuki Sakurai¹

¹*Institute of Theoretical Physics, Faculty of Physics,
University of Warsaw, ul. Pasteura 5, PL-02-093 Warsaw, Poland*

²*Theoretical Physics Department, CERN, CH-1211 Geneva 23, Switzerland*

We show that gauge coupling unification in SUSY models can make a non-trivial interconnection between collider and proton decay experiments. Under the assumption of precise gauge coupling unification in the MSSM, the low energy SUSY spectrum and the unification scale are intertwined, and the lower bound on the proton lifetime can be translated into *upper* bounds on SUSY masses. We found that the current limit on $\tau(p \rightarrow \pi^0 e^+)$ already excludes gluinos and winos *heavier* than ~ 120 and 40 TeV, respectively, if their mass ratio is $M_3/M_2 \sim 3$. Next generation nucleon decay experiments are expected to bring these upper bounds down to ~ 10 and 3 TeV.

Proton decay would be the key evidence for grand unified theories (GUTs) [1]. Among possible decay channels, a special role is played by the $p \rightarrow \pi^0 e^+$ mode for which the dominant contribution may come from the $D = 6$ operators depending almost exclusively on the X, Y boson mass and the unified gauge coupling. This is in contrast to the other channels induced by $D = 5$ operators, which depend on many more parameters, though the rate is typically larger than the $p \rightarrow \pi^0 e^+$ mode.

The main point we want to emphasise and make very explicit in this Letter is that $\tau_{p \rightarrow \pi^0 e^+}$ carries an important information about the low scale supersymmetric (SUSY) spectrum. To this end we assume here that the unification of the gauge couplings is precise (or exact) within the minimal SUSY Standard Model (MSSM) without threshold corrections of GUT scale particles [2]. In fact, there exists a class of models where these corrections are absent or highly suppressed (see e.g. [3]). On the other hand, GUT threshold corrections in conventional models are often too large compared to the typical mismatch of gauge couplings at a high scale in the MSSM (see [4] for a recent discussion). This means that the well-known “*success of gauge coupling unification in the MSSM*”, if not a mere accident, may favour the aforementioned class of models as the correct theory of grand unification.

Under the assumption of precise gauge coupling unification (GCU) in the MSSM, we show that the low energy SUSY spectrum and the unification scale are intertwined, and the lower bound on the proton lifetime $\tau_{p \rightarrow \pi^0 e^+}$ can be translated into *upper* bounds on SUSY masses.* This leads to an interesting interconnection between the proton decay experiments and the collider searches, particularly in view of the future progress on both fronts, in cornering supersymmetric spectrum from above and from below.

At the one-loop the gauge couplings at scale $\tilde{\mu}$ in the

MSSM is given by

$$\frac{2\pi}{\alpha_i(\tilde{\mu})} = \frac{2\pi}{\alpha_i(m_Z)} - b_i \ln\left(\frac{\tilde{\mu}}{m_Z}\right) + s_i. \quad (1)$$

where $\alpha_1 \equiv \frac{3}{5}\alpha_Y$, $i = 1, 2, 3$ represents the gauge group, $b_i = (\frac{33}{5}, 1, -3)$ are the one-loop β -function coefficients for the MSSM and

$$s_i \equiv \sum_{\eta} b_i^{\eta} \ln\left(\frac{m_{\eta}}{m_Z}\right) \quad (2)$$

are the threshold corrections of SUSY particles. For SUSY particle η , the mass and its contribution to b_i are given by m_{η} and b_i^{η} , respectively.

In the special case where all SUSY particles are mass degenerate at M_s , the threshold correction can be written as $s_i = \delta_i \ln(M_s/m_Z)$ with $\delta_i \equiv (b_i - b_i^{\text{SM}})$, where $b_i^{\text{SM}} = (\frac{41}{10}, -\frac{19}{6}, -7)$ are the one-loop β -function coefficients for the Standard Model (SM). In this case, exact gauge unification $\alpha_1(\tilde{\mu}) = \alpha_2(\tilde{\mu}) = \alpha_3(\tilde{\mu}) \equiv \alpha_G^*$ is achieved by the particular values of M_s and $\tilde{\mu}$: $M_s^*, M_G^{\text{deg}*}$, satisfying

$$\frac{2\pi}{\alpha_G^*} - \frac{2\pi}{\alpha_i(m_Z)} + b_i \ln\left(\frac{M_G^{\text{deg}*}}{m_Z}\right) = \delta_i \ln\left(\frac{M_s^*}{m_Z}\right) \quad (3)$$

for all i . It should be kept in mind that the quantities M_s^* , $M_G^{\text{deg}*}$ and α_G^* are not variables but constants defined as the solution to the above three simultaneous equations.

Coming back to the general case, let us decompose the vector s_i into three independent vectors as [7]

$$s_i = \delta_i \ln\left(\frac{T}{m_Z}\right) + b_i \ln \Omega + C. \quad (4)$$

The solution to this set of equations is given by

$$\ln\left(\frac{T}{m_Z}\right) = v_i s_i / D \quad (5)$$

$$\ln \Omega = u_i s_i / D \quad (6)$$

$$C = \epsilon_{ijk} \delta_j b_k s_k / D \quad (7)$$

* Unlike other upper bounds on SUSY masses based on the arguments of the Higgs boson mass [5] or the neutralino relic abundance [6], these bounds dependent neither on the ratio of the Higgs vacuum expectation values, $\tan \beta \equiv v_u/v_d$, nor the assumption of R -parity conservation and the thermal history of the universe.

where summation is understood for the repeated indices and ϵ_{ijk} is the antisymmetric tensor and

$$v = \begin{pmatrix} b_2 - b_3 \\ -b_1 + b_3 \\ b_1 - b_2 \end{pmatrix}, \quad u = \begin{pmatrix} -\delta_2 + \delta_3 \\ \delta_1 - \delta_3 \\ -\delta_1 + \delta_2 \end{pmatrix},$$

$$D = b_2\delta_1 - b_3\delta_1 - b_1\delta_2 + b_3\delta_2 + b_1\delta_3 - b_2\delta_3. \quad (8)$$

Plugging the concrete values of b_i , δ_i and $b_i^?$ into these expressions, one gets

$$T = \left[M_3^{-28} M_2^{32} (\mu^4 m_A)^3 X_T \right]^{\frac{1}{19}}, \quad (9)$$

$$\Omega = \left[M_3^{-100} M_2^{60} (\mu^4 m_A)^8 X_\Omega \right]^{\frac{1}{288}}, \quad (10)$$

$$C = \frac{125}{19} \ln M_3 - \frac{113}{19} \ln M_2 - \frac{40}{19} \ln \mu - \frac{10}{19} \ln m_A$$

$$+ \sum_{i=1, \dots, 3} \left[\frac{79}{114} \ln m_{\tilde{d}_{Ri}} - \frac{10}{19} \ln m_{\tilde{l}_i} - \frac{121}{114} \ln m_{\tilde{q}_i} \right.$$

$$\left. + \frac{257}{228} \ln m_{\tilde{u}_{Ri}} + \frac{33}{76} \ln m_{\tilde{e}_{Ri}} \right]. \quad (11)$$

with

$$X_T \equiv \prod_{i=1, \dots, 3} \left(\frac{m_{\tilde{l}_i}^3}{m_{\tilde{d}_{Ri}}^3} \right) \left(\frac{m_{\tilde{q}_i}^7}{m_{\tilde{e}_{Ri}}^2 m_{\tilde{u}_{Ri}}^5} \right), \quad (12)$$

$$X_\Omega \equiv \prod_{i=1, \dots, 3} \left(\frac{m_{\tilde{l}_i}^8}{m_{\tilde{d}_{Ri}}^8} \right) \left(\frac{m_{\tilde{q}_i}^6 m_{\tilde{e}_{Ri}}}{m_{\tilde{u}_{Ri}}^7} \right). \quad (13)$$

The SUSY mass parameters appearing in this Letter should be understood as the magnitude of the corresponding parameters because phase factors do not affect RG running. In most models, the sfermion contributions to T and Ω are negligible (i.e. $X_T \sim X_\Omega \sim 1$). In particular, these contributions vanish if the masses are degenerate within the SU(5) multiplets, $\mathbf{\bar{5}}_i = (\tilde{d}_{Ri}^c, \tilde{l}_i)$, $\mathbf{10}_i = (\tilde{q}_i, \tilde{u}_{Ri}^c, \tilde{e}_{Ri}^c)_i$. One can explicitly check that for a degenerate spectrum, $\ln \Omega = C = 0$.

To see roles of T , Ω and C in gauge unification, we substitute Eq. (4) into Eq. (1) and obtain

$$\frac{2\pi}{\alpha_i(\tilde{\mu})} = \frac{2\pi}{\alpha_G^*} - b_i \ln \left(\frac{\tilde{\mu}}{\Omega M_G^{\text{deg}^*}} \right) + \delta_i \ln \left(\frac{T}{M_s^*} \right) + C, \quad (14)$$

where Eq. (3) has also been used. It is clear that the exact unification for the general case is obtained when the right-hand-side (RHS) becomes i -independent, that is at $T = M_s^*$ [8] and the exact unification scale is given by

$$M_G = \Omega M_G^{\text{deg}^*}. \quad (15)$$

The unified gauge coupling is related to that of the degenerate case as

$$\alpha_G^{-1} = \alpha_G^{*-1} + \frac{C}{2\pi}. \quad (16)$$

Away from the exact unification, we define a candidate unification scale M_U and a semi-unified coupling

α_U by $\alpha_1(M_U) = \alpha_2(M_U) \equiv \alpha_U$. This scale can be computed from a low energy spectrum as $M_U = \Omega M_G^{\text{deg}^*} (T/M_s^*)^{\frac{\delta_1 - \delta_2}{b_1 - b_2}}$, and at this scale the gauge couplings are given by

$$\frac{2\pi}{\alpha_i(M_U)} = \frac{2\pi}{\alpha_G^*} + \left(\delta_i - b_i \frac{\delta_1 - \delta_2}{b_1 - b_2} \right) \ln \left(\frac{T}{M_s^*} \right) + C. \quad (17)$$

Using this formula, a measure of gauge coupling unification, which we define as $\epsilon_3 \equiv (\alpha_3(M_U) - \alpha_U)/\alpha_U$, is calculated as

$$\epsilon_3 = \frac{\alpha_G^*}{2\pi} Y \ln \left(T/M_s^* \right) + \dots, \quad (18)$$

where the dots represent higher order terms of $\frac{\alpha_G^*}{2\pi}$ and

$$Y \equiv \frac{b_1(\delta_2 - \delta_3) + b_2(-\delta_1 + \delta_3) + b_3(\delta_1 - \delta_2)}{b_1 - b_2}. \quad (19)$$

It is interesting that ϵ_3 depends only on T at the leading order [8].

Our argument so far is based on the one-loop renormalization group equations (RGEs). It turns out that the relations Eqs. (15), (16) and (18) still hold numerically with a good accuracy at two-loop level if the constants are replaced by the two-loop corrected values: $M_s^* = 2.08$ TeV, $M_U^{\text{deg}^*} = 1.27 \cdot 10^{16}$ GeV and $\alpha_G^{*-1} = 25.5$. We show in Fig. 1 the result of our numerical scan. All numerical scans presented in this Letter use a two-loop RGE code including the effect of the top Yukawa coupling, following [9]. We use $\tan \beta = 10$ but a variation of $\tan \beta$ results in negligible effects. The SUSY breaking parameters are uniformly scanned in the logarithmic scale within $[m_{\min}, 10^3$ TeV]. We take $m_{\min} = 1.5$ TeV for M_3 and 200 GeV for M_2, μ and m_A . The sfermion masses are assumed to be universal ($\equiv m_{\tilde{f}}$) for simplicity and $m_{\min} = 1$ TeV is used. We also vary $\alpha_3(m_Z) = 0.1184(7)$, according to the $1\text{-}\sigma$ uncertainty.

The top plot in Fig.1 tests the predicted relation Eq. (18) (dashed line). We see that the exact unification occurs only when the SUSY masses are arranged such that T computed by Eq. (9) is within a certain range [1, 4] TeV centred around ~ 2 TeV. The width of T for exact unification comes mainly from the uncertainty on M_s^* due to the variation of $\alpha_3(m_Z)$.[†] The middle plot shows the correlation between Ω and the exact unification scale, M_G . Hereafter, we require a precise gauge unification, $|\epsilon_3| < 0.1\%$. The dashed line corresponds to Eq. (15). The colour of points represents a typical SUSY scale $\sqrt{M_3 M_2}$. One can see that heavy SUSY tends to have a small unification scale. For the PeV scale SUSY with $\sqrt{M_3 M_2} \sim 10^3$ TeV, M_G is reduced by a factor of 5 compared to the TeV scale one. The bottom plot confirms the predicted relation Eq. (16) (dashed line). The colour-code indicates a

[†] The constants M_s^* , $M_G^{\text{deg}^*}$ and α_G^* should be understood as functions of $\alpha_3(m_Z)$ in the scan.

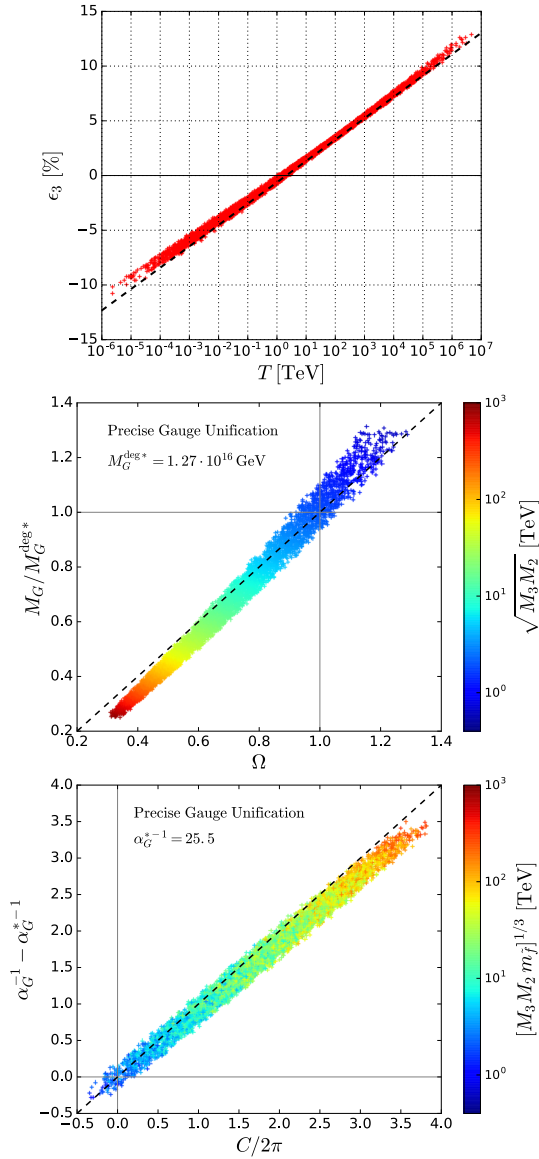


FIG. 1: A scan of SUSY particle masses projected onto the (T, ϵ_3) (top), the $(\Omega, M_G/M_G^{\text{deg}^*})$ (middle) and $(C/2\pi, \alpha_G^{-1} - \alpha_G^{*-1})$ (bottom) planes. In the middle and bottom plots, the precise gauge unification ($|\epsilon_3| < 0.1\%$) is required, and the colour-codes represent typical SUSY scales $\sqrt{M_3 M_2}$ and $(M_3 M_2 m_{\tilde{f}})^{1/3}$, respectively. The dashed lines represent the one-loop relations Eq. (18), (15) and (16) for the top, middle and bottom plots, respectively.

SUSY scale, $(M_3 M_2 m_{\tilde{f}})^{1/3}$. We see that high scale SUSY tends to predict a smaller unified coupling, α_G , but the variation is small and only up to $\sim 10\%$ between the TeV and PeV scale SUSY mass points.

An interesting observation follows from the last two plots of Fig. 1. High scale SUSY, where the unification scale is lower, in general leads to a rapid proton decay, $p \rightarrow e^+ \pi^0$. This is because the rate $\Gamma(p \rightarrow e^+ \pi^0)$ scales as $\alpha_G/(M_G)^4$, where the X, Y boson mass is identified as

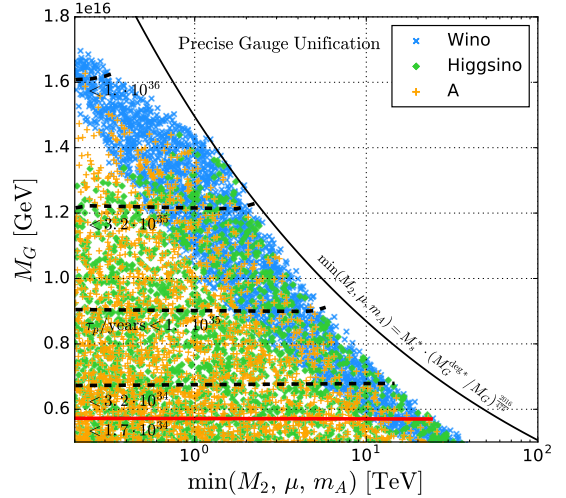


FIG. 2: Points with precise gauge unification projected onto the $\min(M_2, \mu, m_A)$ vs M_G plane. The blue, green and orange points correspond to the points where M_2, μ and m_A is the smallest among them, respectively. The regions below a black-dashed or a red-solid line are excluded by the quoted future or current limits on the proton lifetime. The black-solid line represents the upper bound found at the one-loop level in Eq. (20).

the unification scale, since the precise gauge unification implies all GUT particles charged under the SM gauge group have the same mass, M_G . Turning this around, the lower limit on M_G from the proton lifetime measurement (if found, bearing in mind that the variation of α_G is small) can place *upper bounds* on the masses of SUSY particles. Let us denote this lower limit by M_{PD} : $M_G > M_{PD}$. Then, eliminating M_3 from Eq. (10) by using Eq. (9), Eq. (15) gives us

$$M_2^{4/5} (\mu^4 m_A)^{1/25} < M_s^* \cdot \left(\frac{M_G^{\text{deg}^*}}{M_{PD}} \right)^{20/16} \cdot X_{\text{EW}}^{1/25}, \quad (20)$$

where

$$X_{\text{EW}} \equiv \prod_{i=1 \dots 3} \left(\frac{m_{\tilde{l}_i}}{m_{\tilde{d}_{Ri}}} \right) \left(\frac{m_{\tilde{q}_i}^7}{m_{\tilde{e}_{Ri}}^3 m_{\tilde{u}_{Ri}}^4} \right). \quad (21)$$

This implies that the smallest mass in the LHS is bounded from above by the RHS of Eq. (20). When this bound is saturated, $M_2 = \mu = m_A$. The upper limit on the individual parameters are obtained, for example, as

$$M_2 < M_s^* \cdot \left(\frac{M_s^{*5}}{\mu^4 m_A} \right)^{1/20} \cdot \left(\frac{M_G^{\text{deg}^*}}{M_{PD}} \right)^{504/95} \cdot X_{\text{EW}}^{1/20}. \quad (22)$$

In this expression the RHS is bounded from above by the experimental lower limit on μ and m_A .

The upper bound Eq. (20) is observed in our numerical scan shown in Fig. 2, where the smallest of M_2, μ and m_A is plotted in the x -axis. The blue, green and orange points correspond to the cases where M_2, μ and m_A is

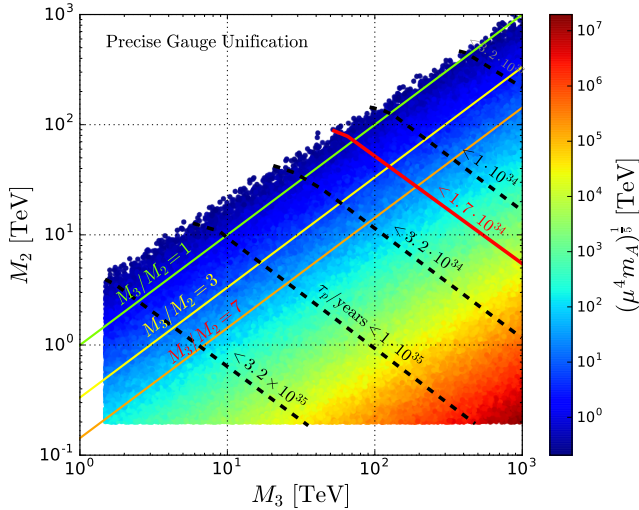


FIG. 3: Points with precise gauge unification projected onto the (M_3, M_2) plane. The colour-code shows $(\mu^4 m_A)^{\frac{1}{5}}$. The regions above the black-dashed and red-solid lines are excluded by the quoted future or current limits on $\tau_{p \rightarrow \pi^0 e^+}$. The three diagonal lines correspond to $R \equiv M_3/M_2 = 1, 3$ and 7 from top to bottom. In this plot the upper boundaries of μ and m_A scans are extended up to 10^7 TeV.

the lightest among the three, respectively. A tendency is observed that M_2 is close to the upper limit if M_2 is the lightest. This is due to the higher power for M_2 in Eq. (20) than for μ and m_A . At each point we calculate $\tau_{p \rightarrow \pi^0 e^+}$ based on [10, 11][‡] using α_G and M_G obtained by the two-loop RGE code. The horizontal black-dashed and red-solid lines represent the boundaries where all points below them have the lifetime shorter than the quoted values. In particular, the region below the red line is excluded by the current limit: $\tau_{p \rightarrow \pi^0 e^+} > 1.7 \cdot 10^{34}$ years [13].

The upper bound on the gluino mass can be found by eliminating $\mu^4 m_A$ in Eq. (10) by using Eq. (9) as

$$M_3 < M_s^* \cdot \frac{M_s^*}{M_2} \cdot \left(\frac{M_G^{\text{deg}^*}}{M_{PD}} \right)^{\frac{216}{19}} \cdot X_{\tilde{g}}^{\frac{1}{4}} \quad (23)$$

with

$$X_{\tilde{g}} \equiv \prod_{i=1 \dots 3} \left(\frac{m_{\tilde{u}_{Ri}} m_{\tilde{e}_{Ri}}}{m_{\tilde{q}_i}^2} \right). \quad (24)$$

As previously, the RHS of Eq. (23) is bounded from above by the experimental lower limit on the wino mass.

If the SUSY breaking mechanism is specified, the ratio of gluino and wino masses is usually predicted. Assuming the value of $R \equiv M_3/M_2$, the following upper bounds can be derived:

$$M_3 < M_s^* \cdot R^{\frac{1}{2}} \cdot \left(\frac{M_G^{\text{deg}^*}}{M_{PD}} \right)^{\frac{108}{19}} \cdot X_{\tilde{g}}^{\frac{1}{8}}, \quad (25)$$

$$(\mu^4 m_A)^{\frac{1}{5}} < M_s^* \cdot R^2 \cdot \left(\frac{M_{PD}}{M_G^{\text{deg}^*}} \right)^{\frac{144}{90}} \cdot X_{\mu}^{\frac{1}{10}}, \quad (26)$$

where

$$X_{\mu} \equiv \prod_{i=1 \dots 3} \left(\frac{m_{\tilde{l}_i}^2}{m_{\tilde{d}_{Ri}}^2} \right) \left(\frac{m_{\tilde{q}_i}^4}{m_{\tilde{e}_{Ri}} m_{\tilde{u}_{Ri}}^3} \right). \quad (27)$$

We show in Fig. 3 our scan in the (M_3, M_2) plane with the colour-code indicating $(\mu^4 m_A)^{\frac{1}{5}}$. As previously, the black-dashed and red-solid lines represent the future and current bounds on $\tau_{p \rightarrow \pi^0 e^+}$. It is evident that M_3 and M_2 are highly sensitive to the proton lifetime and constrained by it from above. This is in direct contrast to collider searches, constraining these parameters from below. Unlike M_3 and M_2 , μ and m_A are almost insensitive to the proton lifetime, which follows from the lower power of M_{PD} in Eq. (26). On the other hand, they are highly sensitive to R . In particular, μ is typically a TeV for $R = 1$ whereas it is $\mathcal{O}(100)$ TeV for $R = 7$. The implication of this to naturalness and phenomenology are studied in detail in [2, 7, 14].

It is remarkable that the current proton lifetime limit already excludes the gluino and wino masses *larger* than 200 and 30 TeV for $R \sim 7$ (e.g. AMSB) and 120 and 40 TeV for $R \sim 3$ (e.g. CMSSM, GMSB), respectively. Next generation nucleon decay experiments are expected to improve the current $\tau_{p \rightarrow \pi^0 e^+}$ limit by a factor of ten [10], which will result in tightening the upper bounds on gluino and wino masses further down to $(M_3, M_2) \lesssim (10, 3)$ TeV for $R \sim 3$ and $(M_3, M_2) \lesssim (15, 2)$ TeV for $R \sim 7$. These bounds are close to the lower mass limits $(M_3, M_2) \gtrsim (10, 2.7)$ TeV [15, 16], which are expected to be obtained at future 100 TeV hadron-hadron colliders.

We have investigated the link between the proton lifetime $\tau_{p \rightarrow \pi^0 e^+}$ and the supersymmetric spectrum under the assumption of vanishing GUT thresholds. It has been shown that most of the allowed mass range of gluinos and winos will be probed by future collider and proton lifetime experiments. It will also be interesting to extend this study to models with non-vanishing GUT threshold corrections (see e.g. [17]).

Acknowledgments

KS thanks Zackaria Chacko, Kiwoon Choi, Sebastian Ellis, Shigeki Matsumoto and James Wells for helpful discussion. The work of SP and KS is partially supported by the National Science Centre, Poland, under research grants DEC-2014/15/B/ST2/02157 and DEC-2015/18/M/ST2/00054. The work of KR and KS is supported by the National Science Centre (Poland) under Grant 2015/19/D/ST2/03136.

-
- [1] For early references see, P. Langacker, Phys. Rept. **72** (1981) 185.
- [2] S. Raby, M. Ratz and K. Schmidt-Hoberg, Phys. Lett. B **687** (2010) 342 [arXiv:0911.4249 [hep-ph]].
- [3] Y. Kawamura, Prog. Theor. Phys. **105** (2001) 999 [hep-ph/0012125]; L. J. Hall and Y. Nomura, Phys. Rev. D **64** (2001) 055003 [hep-ph/0103125]; A. Hebecker and M. Trapletti, Nucl. Phys. B **713** (2005) 173 [hep-th/0411131].
- [4] S. A. R. Ellis and J. D. Wells, Phys. Rev. D **91** (2015) no.7, 075016 [arXiv:1502.01362 [hep-ph]]; S. A. R. Ellis and J. D. Wells, arXiv:1706.00013 [hep-ph].
- [5] G. F. Giudice and A. Strumia, Nucl. Phys. B **858** (2012) 63 [arXiv:1108.6077 [hep-ph]]; M. Ibe and T. T. Yanagida, Phys. Lett. B **709** (2012) 374 [arXiv:1112.2462 [hep-ph]]; E. Bagnaschi, G. F. Giudice, P. Slavich and A. Strumia, JHEP **1409** (2014) 092 [arXiv:1407.4081 [hep-ph]].
- [6] N. Arkani-Hamed, A. Delgado and G. F. Giudice, Nucl. Phys. B **741** (2006) 108 [hep-ph/0601041]; J. Hisano, S. Matsumoto, M. Nagai, O. Saito and M. Senami, Phys. Lett. B **646** (2007) 34 [hep-ph/0610249]; J. Ellis, F. Luo and K. A. Olive, JHEP **1509** (2015) 127 [arXiv:1503.07142 [hep-ph]].
- [7] S. Krippendorf, H. P. Nilles, M. Ratz and M. W. Winkler, Phys. Rev. D **88** (2013) 035022 [arXiv:1306.0574 [hep-ph]].
- [8] M. Carena, S. Pokorski and C. E. M. Wagner, Nucl. Phys. B **406** (1993) 59 [hep-ph/9303202].
- [9] P. Langacker and N. Polonsky, Phys. Rev. D **47** (1993) 4028 [hep-ph/9210235].
- [10] K. S. Babu *et al.*, arXiv:1311.5285 [hep-ph].
- [11] B. Bajc, J. Hisano, T. Kuwahara and Y. Omura, Nucl. Phys. B **910** (2016) 1 [arXiv:1603.03568 [hep-ph]].
- [12] H. Murayama and A. Pierce, Phys. Rev. D **65** (2002) 055009 [hep-ph/0108104].
- [13] V. Takhistov [Super-Kamiokande Collaboration], arXiv:1605.03235 [hep-ex].
- [14] S. Pokorski, K. Rolbiecki, K. Sakurai, *in preparation*.
- [15] T. Cohen, T. Golling, M. Hance, A. Henrichs, K. Howe, J. Loyal, S. Padhi and J. G. Wacker, JHEP **1404** (2014) 117 [arXiv:1311.6480 [hep-ph]].
- [16] M. Low and L. T. Wang, JHEP **1408** (2014) 161 [arXiv:1404.0682 [hep-ph]].
- [17] J. Hisano, T. Kuwahara and N. Nagata, Phys. Lett. B **723** (2013) 324 [arXiv:1304.0343 [hep-ph]].